Development 133, 1231-1240 (2006) doi:10.1242/dev.02299

Steroid hormone-dependent transformation of *polyhomeotic* mutant neurons in the *Drosophila* brain

Jian Wang[1,*], Ching-Hsien J. Lee[2,*], Suewei Lin[3] and Tzumin Lee[3,†]

Polyhomeotic (Ph), which forms complexes with other Polycomb-group (PcG) proteins, is widely required for maintenance of cell identity by ensuring differential gene expression patterns in distinct types of cells. Genetic mosaic screens in adult fly brains allow for recovery of a mutation that simultaneously disrupts the tandemly duplicated *Drosophila ph* transcriptional units. Distinct clones of neurons normally acquire different characteristic projection patterns and can be differentially labeled using various subtype-specific drivers in mosaic brains. Such neuronal diversity is lost without Ph. In response to ecdysone, *ph* mutant neurons are transformed into cells with unidentifiable projection patterns and indistinguishable gene expression profiles during early metamorphosis. Some subtype-specific neuronal drivers become constitutively activated, while others are constantly suppressed. By contrast, loss of other PcG proteins, including Pc and E(z), causes different neuronal developmental defects; and, consistent with these phenomena, distinct Hox genes are differentially misexpressed in different PcG mutant clones. Taken together, *Drosophila* Ph is essential for governing neuronal diversity, especially during steroid hormone signaling.

KEY WORDS: *Polyhomeotic*, Polycomb group, Neuronal cell fate maintenance, Ecdysone, Metamorphosis

INTRODUCTION

Development of nervous systems involves derivation of numerous distinct subtypes of neurons from limited numbers of precursors (reviewed by Doe and Skeath, 1996). Cells imprint histories of development in their genomes; and differential imprinting of genomes is fundamental to cell differentiation (reviewed by Orlando, 2003). The Polycomb group (PcG) of nuclear proteins, including Polyhomeotic (Ph), is known to modulate gene expression globally in the genomes according to their patterns of imprinting (reviewed by Pirrotta, 1998; Beuchle et al., 2001). However, little progress has been made to elucidate roles of PcG proteins in neuronal development since the initial characterization of the neural phenotypes of *ph* mutants 17 years ago (Smouse et al., 1988).

Neural tissues differentiate step by step. First, distinct neuronal precursors, characterized with different transcriptional codes, are specified during patterning of neuroectoderm (Briscoe et al., 2000; Urbach et al., 2003). Second, distinct precursors further give rise to different characteristic sets of multiple subtypes of neurons during neurogenesis (Lee et al., 1999; Schmid et al., 1999; Jefferis et al., 2001). Both processes of cell diversification involve spatial and/or temporal patterning of tissues (reviewed by Jacob and Briscoe, 2003; Zhong, 2003). Tissue patterning permits acquisition of different gene expression profiles in originally equivalent cells, while maintenance of cell type-specific transcription programs depends on various mechanisms of epigenetic functions (Orlando, 2003).

Much of our knowledge about roles of epigenetic imprint in cell differentiation comes from characterization of several PcG genes that were originally identified through mutant screens based on derepression of homeotic (Hox) genes in *Drosophila* embryos (e.g. Lewis, 1978; Duncan, 1982; Jurgens, 1985). Proper patterning of *Drosophila* embryos requires expression of distinct Hox genes in different spatially restricted regions along the anteroposterior axis (e.g. McGinnis and Krumlauf, 1992). Expression of Hox genes is initially controlled by the Gap proteins, such as Hunchback and Kruppel, which set the limits of Hox gene expression by repressing transcription during early embryogenesis (reviewed by Bienz and Muller, 1995). Interestingly, such repression of Hox genes lasts through cell divisions and in the absence of the Gap repressors. Heritable silencing of Hox genes at the later developmental stages requires PcG proteins (e.g. Lewis, 1978; Duncan, 1982; Jurgens, 1985; Bienz and Muller, 1995). Both the Hox genetic system and its late epigenetic maintenance exist in higher organisms (e.g. Gould, 1997; Forlani et al., 2003). PcG proteins, thus, constitute a widely conserved cell memory system that prevents changes in cell identity by maintaining transcriptional repression of previously suppressed genes throughout development and in adulthood.

PcG proteins are thought to maintain gene silencing by controlling chromatin accessibility (e.g. Boivin and Dura, 1998; Zink and Paro, 1995; Fitzgerald and Bender, 2001). In vivo, different PcG proteins form at least two distinct multimeric chromatin silencing complexes (Ng et al., 2000). The PRC1 complex, containing Polycomb (Pc) and Polyhomeotic (Ph) among others, appears physically associated with the chromatin of specific cis-regulatory sequences in Hox genes, called Polycomb response elements (PREs) (e.g. Shao et al., 1999; Saurin et al., 2001; Horard et al., 2000; Bloyer et al., 2003; Ringrose et al., 2003). Meanwhile, experiments with DNA-tethered PcG proteins, such as *GAL4-Pc*, have provided evidence that PcG proteins function as potent transcriptional repressors (Muller, 1995). But detailed molecular links remain missing from binding of PcG complexes with PREs to chromatin remodeling and transcriptional silencing. It is also unclear how transiently expressed factors help chromatin silencing complexes find their way onto targets and how these complexes retain characteristic chromatin-binding patterns from one cell generation to the next. In addition, evidence accumulates to challenge our conventional views on the biological functions of PcG.

[1]Department of Entomology, University of Maryland, College Park, MD 20742, USA. [2]Division of Hematology Oncology, Department of Medicine, University of Massachusetts Memorial Medical Center, Worcester, MA 01655, USA. [3]Department of Neurobiology, University of Massachusetts Medical School, Worcester, MA 01605, USA.

*These authors contributed equally to this work
†Author for correspondence (e-mail: tzumin.lee@umassmed.edu)

Accepted 24 January 2006

First, several PcG proteins seem to have a dual role in both repression and activation of transcription, depending on the locus and genetic context (Brock and van Lohuizen, 2001). Second, distinct PcG proteins function in different complex manners. Some PcG proteins are differentially distributed from others on polytene chromosomes (DeCamillis et al., 1992; Franke et al., 1992; Ng et al., 2000); and the phenotypes of different PcG mutants are distinct (e.g. Campbell et al., 1995; Narbonne et al., 2004). Finally, derepression of Hox genes is variably involved in different mutants and in distinct tissues (e.g. Beuchle et al., 2001; Dura and Ingham, 1988; Simon et al., 1992; Choi et al., 2000).

Although global misrouting of CNS axons has been well demonstrated in *ph* mutant embryos (Smouse and Perrimon, 1990), little is known about roles of PcG complexes in specific neuronal developmental processes. Here, we report recovery of a new *ph* recessive lethal mutation from genetic mosaic screens in adult fly brains. Loss of subtype identity was evident in *ph* mutant clones within otherwise phenotypically wild-type brains. Through metamorphosis, all *ph* mutant neurons were transformed into cells with unidentifiable projection patterns and indistinguishable gene expression profiles. But postembryonic-born *ph* mutant neurons were never transformed without experiencing the prepupal ecdysone peak. In addition, we detected limited derepression of Hox genes in *ph* mutant neurons and requirement of distinct PcG proteins for different aspects of neuronal development. Taken together, we demonstrate that *Drosophila* Ph plays an essential role in maintaining neuronal diversity through metamorphosis, showing possible two-way interactions between steroid hormone signaling and the epigenetic functions of PcG.

MATERIALS AND METHODS

Fly strains

Creation of *l(X)MB342* MARCM clones involves: (1) *FRT19A,hs-FLP,tubP-GAL80;UAS-mCD8GFP;GAL4-OK107*; (2) *UAS-mCD8GFP,GAL4-NP225*; (3) *ato-GAL4* (Hassan et al., 2000); and (4) *elav-GAL4* (Luo et al., 1994). (5) *FRT19A, UAS-mCD8GFP* was used to create wild-type MARCM clones. (6) Pc^{XT109}*,FRT2A/TM6C* and (7) $E(z)^{731}$*,FRT2A/Tm6C* were used together with (8) *hs-FLP,UAS-mCD8GFP;FRT2A,tubP-GAL80;GAL-OK107*, (9) *GAL4-C155,UAS-mCD8GFP,hs-FLP* and (10) *FRT2A,tubP-GAL80* to create *Pc* and *E(z)* MARCM clones. Fly stocks used for mapping the mutations include (11) *ec,cv,ct,t/C(1)DX* (BL-1163), (12) *y,ct,ras,f* (BL-4362), (13) *Df(1)64c18,g,sd/Dp(1;2;Y)w[+]/C(1)DX* (BL-936), (14) *Dp(1;f)R/y,dor* (BL-761), (15) *Df(1)w258-45/C(1)DX; Dp(1;3)w[vco]* (BL-1527), (16) *Df(1)Pgd-kz* (BL-1902), (17) *Df(1)Pgd35* (BL-1986), $wapl^{2}$ (BL-5741), (18) ph^{602} (BL-5444), (19) Pgd^{G0385} (BL-11998) and (20) *l(1)G0458* (BL-10112). Phenotypic rescue was carried out with (21) *P*{*ph-d*$^{+}$} transgene that comprises the *ph-d* transcription unit (Randsholt et al., 2000).

MARCM-based genetic screens

Our ongoing genetic mosaic screens have been reported before (Lee et al., 2000; Wang et al., 2002; Zheng et al., 2003). Briefly, MARCM clones of MB neurons, which are homozygous for EMS-mutagenized various chromosome arms, were created and screened for abnormal neurogenesis or neuronal morphogenesis. Mutant chromosomes with interesting phenotypes were then recovered for future analysis.

Mapping by recombination and complementation

After learning that the *l(X)MB342* line was homozygous lethal, we first mapped the lethal mutation(s) using linkage analysis. Homologous recombination was induced between the *FRT19A*, *UAS-mCD8-GFP* mutant chromosome and an X chromosome carrying multiple visible mutations. Hemizygous male progeny were collected and analyzed for viable recombination patterns. Based on the recombination patterns, *l(X)MB342* mutation(s) should be between y (1A5) and *w* (3C1). Three duplications, *Dp(1;f)R*, *Dp(1;2;Y)w[+]*, and *Dp(1;3)w[vco]*, were found to rescue the lethality caused by homozygous *l(X)MB342*. *Dp(1;2;Y)w[+]* rescued *l(X)MB342* males were used to conduct complementation tests with related deficiency or mutant lines.

Induction and phenotypic analysis of MARCM clones

Following induction of mitotic recombination at selected stages, MARCM clones of GAL80-minus cells were created from heterozygous precursors and examined at various later stages. Organisms were dissected in cold phosphate-buffered saline and their brains were fixed and immunostained, as previously described (Lee and Luo, 1999). MARCM clones were detected by the rat anti-mCD8 mAb (1:100, Caltag). Immunofluorescent signals were collected by confocal microscopy and then processed using Adobe Photoshop.

Immunohistochemistry

Fly brains were fixed and subjected to immunostaining following the procedures as described previously (Lee et al., 1999). Rabbit polyclonal antibodies against Lab (1:100), Pb (1:100) and Dfd (1:30) were kindly supplied by T. Kaufman. The mouse monoclonal antibodies anti-Abd-A (1:400) and anti-Ubx (1:30) were gifts from I. Duncan and J. Müller, respectively. Other mouse monoclonal antibodies used in this study, including anti-Abd-B (1A2E9) (1:100), anti-Antp (8C11) (1:100) and anti-Scr (6H4.1) (1:100), were obtained from the Developmental Studies Hybridoma Bank developed under Department of Biological Sciences, Iowa City, IA 52242.

CNS organ culture

The culture protocol was adopted from Gibbs and Truman (Gibbs and Truman, 1998). Briefly, the CNSs were dissected from mid-third instar larvae and, following removal of the ring glands, cultured in 200 μl of the Shield & Sang M3 *Drosophila* medium (Sigma) containing 7.5% heat-inactivated fetal calf serum (Gibco) and 1% of penicillin (10,000 units/ml)-streptomycin (10 mg/ml) solution (Sigma). Cultures were kept in a 25°C humidified culture incubator and aerated with a mixture of 95% air and 5% CO_2. Culture medium was changed every 48 hours. 20-hydroxyecdysone (20E) (Sigma) was dissolved in isopropanol with a concentration of 10 mg/ml to serve as a storage solution. A final concentration of 1 μg/ml 20E was achieved by adding this storage solution directly into culture medium. The same amount of isopropanol was added into the culture medium in the control experiments. After culture, the CNS was fixed in 4% paraformaldehyde in PBS.

RESULTS

Loss of Ph accounts for presence of multiple unrecognizable MARCM clones of *l(X)MB342* mutant neurons

With various GAL4 drivers, MARCM technologies allow for labeling of distinct specific clones of GAL80-minus neurons in otherwise GAL80 heterozygous brains (Lee and Luo, 1999). For example, using *GAL4-OK107* (Connolly et al., 1996) in MARCM, one can selectively label clones of GAL80-minus neurons in the *Drosophila* olfactory learning/memory center, the mushroom bodies (MBs) (e.g. Lee et al., 1999). The MBs are paired neuropils (Fig. 1A). One MB is derived from four neuroblasts (Nbs), each of which continuously undergoes asymmetric divisions to produce a similar set of MB neurons through different developmental stages until fly eclosion (Ito et al., 1997; Lee et al., 1999). In the presence of *GAL4-OK107*, when mitotic recombination results in loss of GAL80 from one MB Nb, one would observe labeling of all the MB neurons subsequently derived from the GAL80-minus MB Nb (Fig. 1B). One MB Nb clone, generated in newly hatched larvae, consists of about 400 neurons at the adult stage and exhibits all basic MB morphological features. MB cell bodies are clustered on the posterior dorsal surface of the protocerebrum. Their dendrites elaborate immediately below cell bodies and constitute the calyx. Axons then project through the peduncle into various subsets of MB lobes (Fig. 1B).

To identify genes governing various aspects of neuronal development, we have been generating MARCM clones of MB neurons that are homozygous for various mutations in otherwise largely heterozygous organisms (Lee et al., 2000; Wang et al., 2002; Zheng et al., 2003). Following chemical mutagenesis, we screened about 800 X chromosomes (Fig. 1C) and recovered one mutated X chromosome that drastically altered the general patterns of MARCM clones (Fig. 1D). We no longer observed typical MB clones. Instead, there were multiple unrecognizable clones of cells in the mosaic brains. It appears that clones of homozygous mutant neurons undergo very rudimentary morphogenesis and fail to acquire any specific projection patterns (Fig. 1D). In addition, homozygous mutant cells might constitutively express GAL4 (see below), resulting in ubiquitous labeling of GAL80-minus clones despite use of a MB-selective GAL4 driver.

The mutant stock is homozygous lethal and probably carry one lethal mutation, *l(X)MB342*, responsible for most of the abnormal phenotypes. To determine how many lethal hits actually exist and roughly map where *l(X)MB342* might be located, we conducted linkage analysis based on recombination patterns and frequencies between the hemizygous lethal phenotype and multiple X-chromosome recessive visible markers (see Materials and methods). We detected only one X-chromosome lethal hit around the 2 to 3 cytogenetic region. Presence of *l(X)MB342* in the 2 to 3 cytogenetic region was further confirmed by rescuing hemizygous males with several duplicated genomic fragments spanning the 2 to 3 cytogenetic domain. Complementation experiments were then made possible between the rescued *l(X)MB342* hemizygous male flies and various deficiency lines. We thus mapped the *l(X)MB342* mutation to the interval between 2D3 and 2E1 (Fig. 2A). Saturated mutagenesis followed by detailed genetic analysis has previously revealed five lethal complementation groups around this region (Perrimon et al., 1985). Interestingly, *l(X)MB342* fails to complement with three of the five lethal groups. It appears that *ph*, *PgD* and *wapl*, which are located within a 40 kb genomic segment, are all mutated in the *l(X)MB342* mutant X chromosome (Fig. 2A). However, no deletion could be detected in any of these open reading

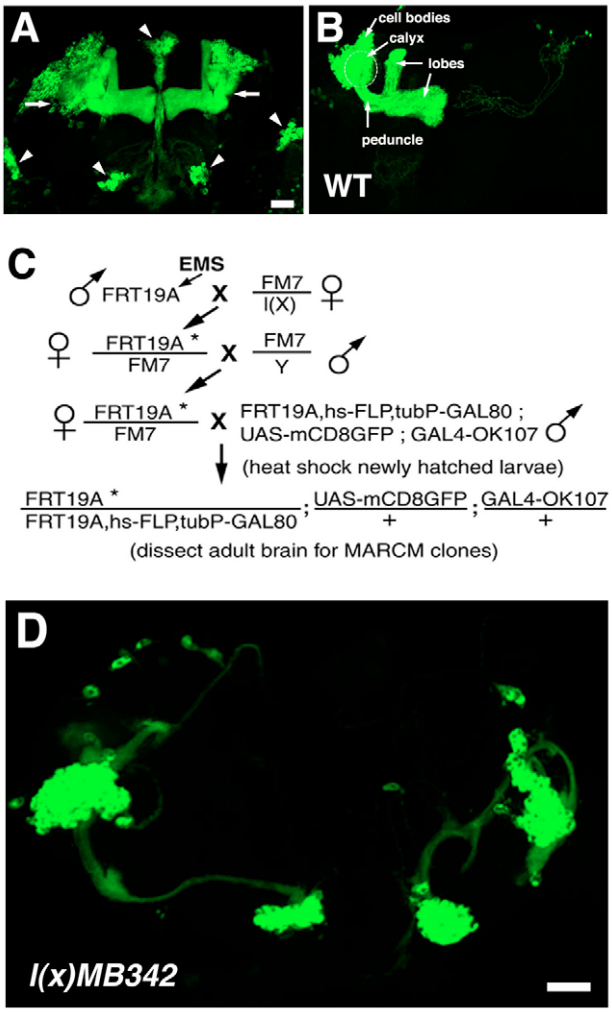

Fig. 1. Identification of *l(X)MB342* based on presence of ectopic unrecognizable MARCM clones. (**A**) Composite confocal images of an adult brain showing labeling of the paired MBs by *GAL4-OK107*-driven expression of *mCD8-GFP* (arrows). *GAL4-OK107* labels a few non-MB structures in the central brain (arrowheads). (**B**) Composite confocal images of a wild-type mosaic adult brain showing one MB Nb clone in the left hemisphere and multiple single-cell/two-cell clones of MB neurons in the right hemisphere. (**C**) Summary of the genetic crosses for the MARCM-based genetic screen. The star represents a mutagenized chromosome. (**D**) Composite confocal images of a mosaic adult brain containing clones of *l(X)MB342* homozygous mutant neurons. Multiple ectopic clones with rudimentary projections are present. Clones were induced in newly hatched larvae unless otherwise indicated. Scale bar: 20 μm. Genotypes: (A) *UAS-mCD8-GFP/+;GAL4-OK107/+;* (B) *FRT19A/FRT19A,hs-FLP,tubP-GAL80;UAS-mCD8-GFP/+;GAL4-OK107/+*; and (D) *FRT19A,l(X)MB342/FRT19A,hs-FLP,tubP-GAL80;UAS-mCD8-GFP/+;GAL4-OK107/+*.

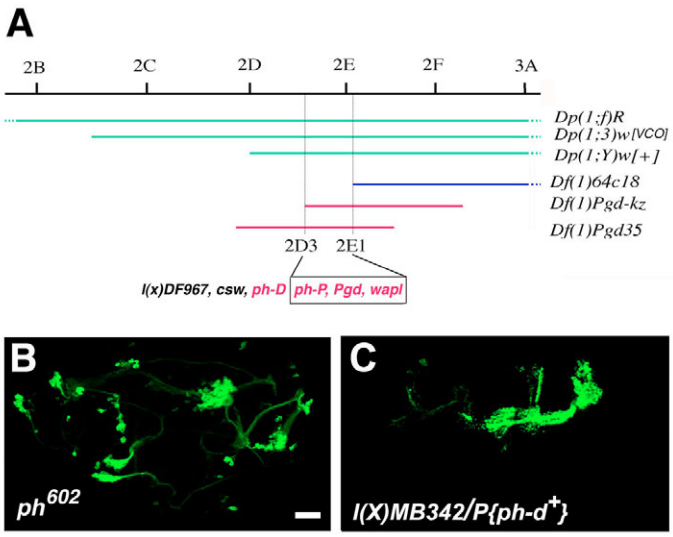

Fig. 2. Loss of Ph accounts for *l(X)MB342* mutant phenotypes. (**A**) *l(X)MB342* carries a lethal mutation within the internal 2D3 to 2E1, defined by the distal breaking points of *Df(1)64c18* and *Df(1)Pgd-kz*. All rescuing regions of duplication are shown in green, while the *l(X)MB342*-complemented (purple) and *l(X)MB342*-non-complemented (red) deleted segments are shown. In addition, three (in red) out of five lethal complementation groups around this region failed to complement with *l(X)MB342*. (**B**) Composite confocal images of a mosaic adult brain containing MARCM clones of ph^{602} homozygous mutant neurons. Phenotypes are similar to *l(X)MB342* mutant clones shown in Fig. 1D. (**C**) Composite confocal images of a mosaic adult brain containing $P\{ph\text{-}d^{+}\}$-rescued *l(X)MB342* mutant neuronal clones. Genotypes: (B) *FRT19A,*ph^{602}*/FRT19A,hs-FLP,tubP-GAL80;UAS-mCD8-GFP/+;GAL4-OK107/+*; and (C) *FRT19A,l(X)MB342/FRT19A,hs-FLP,tubP-GAL80;UAS-mCD8-GFP/+;*$P\{ph\text{-}d^{+}\}$*/+;GAL4-OK107/+*. Scale bar: 20 μm.

frames (data not shown). Furthermore, we found that a lethal P-element line, *l(1)G0458* (BL-10112), that carries a P-element insertion within the promoter region of *ph-D* (Peter et al., 2002), also fails to complement with *ph*, *PgD* and *wapl* mutations, suggesting possible presence of a local cis element essential for normal expression of several contiguous genes.

To identify which gene(s) are primarily involved in causing *l(X)MB342* phenotypes, we conducted MARCM analysis for various known mutations, including ph^{602}, PgD^{G0385} and $wapl^{2}$. Among them, only ph^{602} allows us to obtain multiple unrecognizable clones of GAL4-positive and GAL80-minus cells after transient induction of mitotic recombination in newly hatched larvae. MARCM clones of ph^{602} mutant cells grossly phenocopy *l(X)MB342* mutant clones (Fig. 2B). *Ph* gene extends over a 28.6 kb genomic fragment and comprises two independent transcription units, *ph* proximal (*ph-p*) and *ph* distal (*ph-d*), which are direct tandem duplication (Dura et al., 1987). ph^{602} is a null *ph* allele that carries a 2 kb deletion in *ph-d* and a complex genomic DNA rearrangement involving both deletion and inversion in *ph-p* (Boivin et al., 1999). Interestingly, a transgene that specifically encodes Ph-d, $P\{ph\text{-}d^{+}\}$ can largely rescue the mutant phenotypes of *l(X)MB342* clones (Fig. 2C). This is not only consistent with the notion that Ph-P and Ph-D are functionally redundant (Dura et al., 1987; Deatrick et al., 1991; Saget and Randsholt, 1994), but also suggest further that loss of Ph functions accounts for most, if not all, of the observed *l(X)MB342* phenotypes. To examine specifically roles of Ph proteins in development of distinct neurons, we selectively focused phenotypic analysis on clones of ph^{602} mutant neurons hereafter.

Ph is required for proper neuronal morphogenesis as well as establishment of cell type-specific gene expression patterns

In insect brains, postmitotic neurons of the same lineages often remain associated; and distinct clones of neurons normally acquire different characteristic projection patterns (e.g. Fig. 1A,B; Fig. 3A,D,I,L). One can, thus, describe different clones of neurons based on the cell body positions and neurite trajectories of individual clones. Although most *GAL4-OK107*-labeled *ph* mutant neurons exist in discrete clones, we are no longer able to determine clonal identity because of a lack of recognizable neuropil structural features in the *ph* mutant clones. In addition, without Ph, the MB GAL4 driver, *GAL4-OK107*, appears labeling more GAL80-minus clones than it usually does (Fig. 3N, compared with 3J). In wild-type mosaic brains, *GAL4-OK107* labels about 0.75±0.23 neuroblast clones per brain; and the majority of these clones consist of MB neurons. By contrast, there are 8.56±2.44 clones of *ph* mutant neurons per brain that could be labeled by *GAL4-OK107* after comparable induction of mitotic recombination.

To gain additional insights into the neuronal functions of Ph, we repeated MARCM analysis of ph^{602} using various GAL4 drivers. Different GAL4 drivers normally label different types of MARCM clones, depending on GAL4 expression patterns. Thus, while the pan-neuronal *elav-GAL4* (Luo et al., 1994) allows for visualization of all neuronal clones, *GAL4-OK107* (Connolly et al., 1996), *GAL4-NP225* (gift from K. Ito), *ato-GAL4* (Hassan et al., 2000) and *GAL4-EB1* (Wang et al., 2002) selectively label clones of MB neurons, antennal lobe projection neurons (PNs), Atonal-positive dorsal cluster (DC) neurons and specific ellipsoid body (EB) neurons, respectively, in wild-type mosaic brains (Fig. 3I-L; data not shown for *GAL4-EB1*). Interestingly, when such distinct GAL4 drivers were individually used to label *ph* mutant clones, we detected either all or none of *ph* mutant clones (Fig. 3M-P). First of all, similar numbers of *elav-GAL4*-labeled clones exist between wild-type (8.85±3.15) and *ph* (9.12±2.79) mosaic brains, suggesting that *ph* mutation does not affect patterns of mitotic recombination or initial neurogenesis (compare Fig. 3I with 3M). Second, *GAL4-OK107* and *GAL4-NP225* label similar numbers of *ph* mutant clones (8.56±2.44 and 7.87±2.62, respectively) as the pan-neuronal *elav-GAL4* does, probably owing to ectopic activation of these GAL4 drivers in all *ph* mutant neurons (compare Fig. 3N and 3O with 3M). Third, *ato-GAL4* and *GAL4-EB1*, by contrast, become suppressed and fail to label any *ph* mutant cells in adult mosaic brains (Fig. 3P). In summary, we no longer detect differential GAL4 expression in *ph* mutant neurons of various origins. Moreover, instead of acquiring different characteristic projections, distinct clones of *ph* mutant neurons are typically found with similar simple bundles of neurites (Fig. 3M-O). Endogenous genes may also display either ubiquitous or no expression in *ph* mutant clones, as evidenced by lack of fasciculin II (Lin and Goodman, 1994) expression (based on immunostaining with the 1D4 monoclonal Ab) in all the examined *ph* mutant clones (data not shown). These phenomena collectively suggest that *ph* mutant neurons lose their individual identities and are uniformly transformed into indistinguishable abnormal cells.

Regulation of gene expression by PcG complexes is thought to occur via changes in local chromatin structures (reviewed by Levine et al., 2004). We wondered whether derepression versus inactivation of a given GAL4 driver depends on its specific genomic locus. Jumping an existing *ato-GAL4* transgene out of its original chromosome, we isolated 10 additional independent *ato-GAL4* drivers that maintain strong GAL4 expression in Ato-positive CNS neurons but probably have the *ato-GAL4* transgene inserted in 10 different genomic domains. We observe that none of these independent *ato-GAL4* drivers is capable of labeling *ph* mutant neurons in adult mosaic brains, yielding no evidence for involvement of local chromatin structures in constitutive silencing of *atonal*. Instead, silencing of *ato-GAL4* in *ph* mutant neurons possibly occurs following derepression of some *ato-GAL4* repressor(s).

Remarkably, the aforementioned *ph* mutant phenotypes are not observed prior to pupal formation. First, in mosaic larval brains, most subtype-specific GAL4 drivers label different characteristic *ph* mutant clones. For example, although *GAL4-NP225* failed to label anything (Fig. 3G), *GAL4-OK107* and *ato-GAL4* selectively labeled MB and DC clones, respectively (Fig. 3F,H). These observations suggest that derepression of *GAL4-OK107* and inactivation of *ato-GAL4* in *ph* mutant neurons must occur later. Second, despite various degrees of morphological defects, distinct mutant clones roughly retained their normal patterns of projections at the wandering larval stage (Fig. 3E-H compare with 3A-D). Thus, *ph* mutant neurons remain largely recognizable until sometime after pupal formation. What a coincident for the loss of neuronal subtype identity to take place during metamorphosis when the prepupal ecdysone peak activates various transcriptional hierarchs in distinct types of cells.

Ecdysone-dependent transformation of *ph* mutant neurons during early metamorphosis

If *ph* mutant neurons gradually transform regardless of ecdysone-mediated metamorphosis, one would observe similar phenotypes in all aged *ph* mutant clones no matter whether they were induced before or after the prepupal ecdysone peak. To examine possible involvement of ecdysone signaling in Ph-dependent maintenance of neuronal diversity, we generated clones of *ph* mutant neurons at late

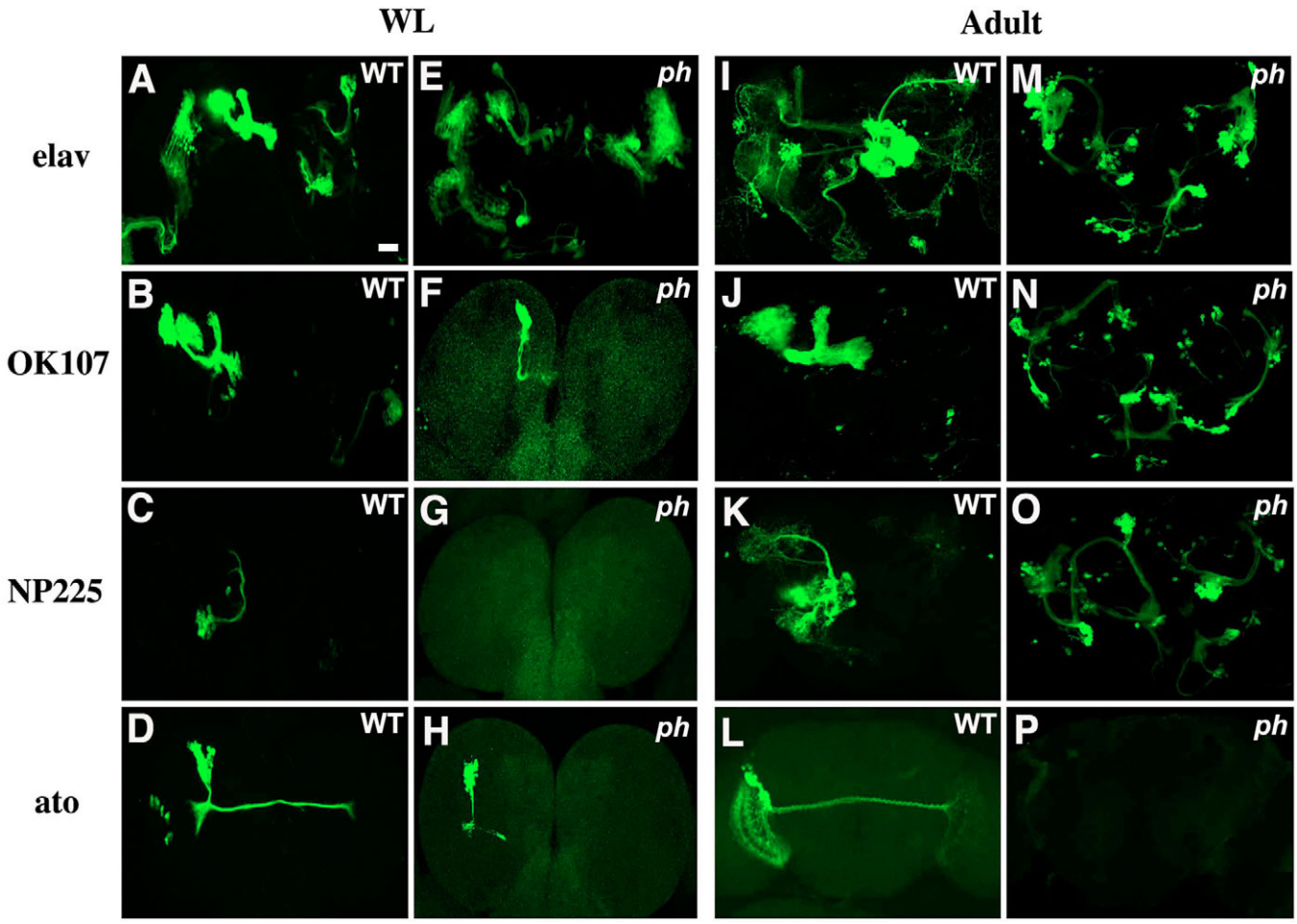

Fig. 3. MARCM analysis of *ph*, using various GAL4 drivers, before and after metamorphosis. Composite confocal images of mosaic brains examined at the wandering larval (WL) (**A-H**) or adult (**I-P**) stages. MARCM clones of wild-type or *ph* mutant neurons were labeled using various GAL4 drivers. (A-D,I-L) In wild type, different GAL4s permit labeling of distinct types of neurons before metamorphosis (A-D), and usually the labeling patterns are preserved at the adult stage (I-L). (E-H) Before metamorphosis, various GAL4 drivers label different clones of *ph* mutant neurons; distinct *ph* mutant clones, like their wild-type controls (A-D), acquire different characteristic projection patterns. (M-P) By contrast, at the adult stage, *GAL4-OK107* (N) and *GAL4-NP225* (O), like the pan-neuronal driver *elav-GAL4* (M), labels many clones, while *ato-GAL4* is completely suppressed (P). Moreover, without characteristic projection patterns, *ph* mutant clones are no longer identifiable in adult brains. Genotypes: (A,I) *FRT19A/FRT19A,hs-FLP,tubP-GAL80;UAS-mCD8-GFP/+;elav-GAL4/+*; (E,M) *FRT19A,ph^{602}/FRT19A,hs-FLP,tubP-GAL80;UAS-mCD8-GFP/+;elav-GAL4/+*; (B,J) *FRT19A/FRT19A,hs-FLP,tubP-GAL80;UAS-mCD8-GFP/+;GAL4-OK107/+*; (F,N) *FRT19A,ph^{602}/FRT19A,hs-FLP,tubP-GAL80;UAS-mCD8-GFP/+;GAL4-OK107/+*; (C,K) *FRT19A/FRT19A,hs-FLP,tubP-GAL80;UAS-mCD8-GFP/GAL4-NP225*; (G,O) *FRT19A,ph^{602}/FRT19A,hs-FLP,tubP-GAL80;UAS-mCD8-GFP/GAL4-NP225*; (D,L) *FRT19A/FRT19A,hs-FLP,tubP-GAL80;UAS-mCD8-GFP/ato-GAL4;* (H,P) *FRT19A,ph^{602}/FRT19A,hs-FLP,tubP-GAL80;UAS-mCD8-GFP/ato-GAL4*. Scale bar: 20 μm.

larval versus early pupal stages and checked their phenotypes 2 days and 2 weeks after eclosion. As expected, we obtained many clones within the optic lobes upon induction of mitotic recombination at the mid-3rd instar stage when optic lobe (OL) precursors were actively dividing (Fig. 4A). Distinct GAL4 drivers were again used to probe neuronal cell fates. For example, all *GAL4-OK107*-labeled OL cells are negative for *GAL4-NP225* expression in wild-type mosaic brains (compare Fig. 4A with 4B). By contrast, OL clones of *ph* mutant neurons are positive for both *GAL4-OK107* and *GAL4-NP225* expression (Fig. 4C,D). Additional phenotypes are observed in the morphologies of *ph* mutant OL clones. For example, most mutant OL neurons are aberrantly aggregated and their bundled neurites fail to defasciculate into any recognizable optic lobe neuropils (Fig. 4C,D). We thus conclude that all the *ph* mutant neuronal clones generated prior to pupal formation have lost their original identities and evolved into undistinguishable clones at the adult stage. We then generated MARCM clones 1 day after pupal formation and, by great contrast, detected no indication for similar cell fate transformation even in much aged *ph* mutant neurons. MB Nbs, different from other Nbs, continue producing post-mitotic neurons through the entire pupal life and can be subject to mitotic recombination until eclosion (Lee et al., 1999). Unlike *ph* mutant OL clones, pupal-born MARCM clones of *ph* mutant MB neurons are strongly labeled by *GAL4-OK107* while remaining negative for *GAL4-NP225* expression, even in 2-week-old adults (compare Fig. 4G with 4H). In addition, we see no problem in identifying pupal-born *ph* mutant MB neurons. They acquired basic MB neuronal trajectories despite subtle morphogenetic defects (Fig. 4G), reminiscent of larval-born *ph* mutant MB neurons examined before pupal formation (Fig. 3F). Taken together, these observations suggest that *ph* mutant neurons lose their subtype-characteristic gene expression and neurite projection patterns specifically during metamorphosis.

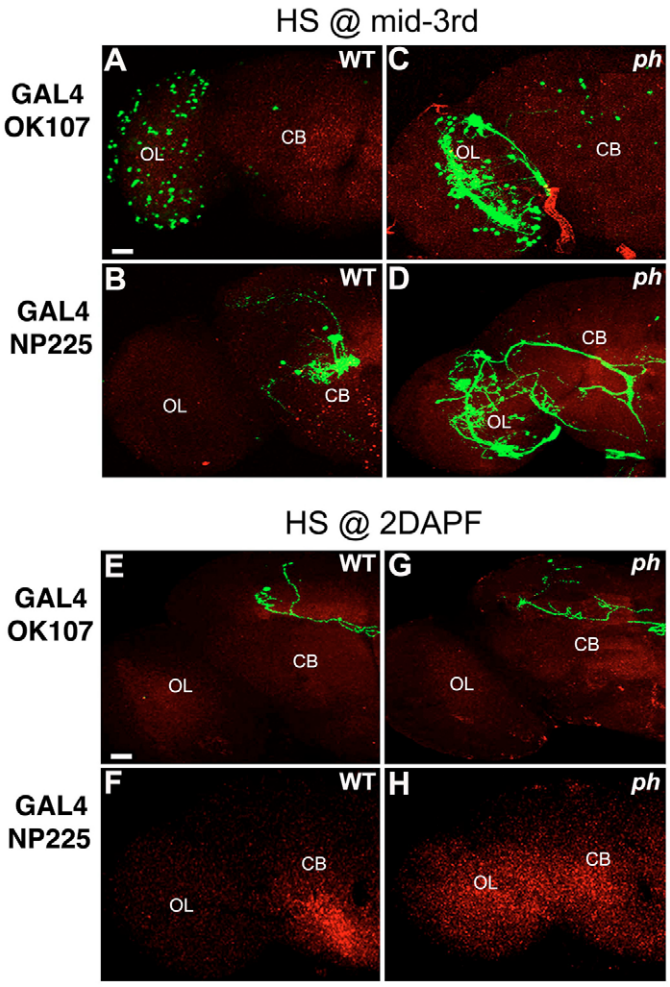

Fig. 4. *ph* mutant clones, induced before versus after the prepupal ecdysone peak, exhibit distinct phenotypes. Composite confocal images of mosaic adult brains containing clones of wild-type or *ph* mutant neurons that were induced at the mid-3rd instar stage (**A-D**) or two days after pupal formation (2D APF) (**E-H**). (A,B,E,F) Wild-type brains exhibit different patterns of clones with *GAL4-OK107* (A,E) versus *GAL4-NP225* (B,F). (C,D) Both GAL4s labeled analogous *ph* mutant clones following induction of mitotic recombination at the mid-3rd instar stage. (G,H) By contrast, *GAL4-OK107* (G), but not *GAL4-NP225* (H), permits labeling of mid-pupa-born *ph* mutant MB neurons. Genotype: (A,E) *FRT19A/FRT19A,hs-FLP,tubP-GAL80;UAS-mCD8-GFP/+;GAL4-OK107/+*; (C,G) *FRT19A,ph^{602}/FRT19A,hs-FLP,tubP-GAL80;UAS-mCD8-GFP/+;GAL4-OK107/+*; (B,F) *FRT19A/FRT19A,hs-FLP,tubP-GAL80;UAS-mCD8-GFP/GAL4-NP225*; (D,H) *FRT19A,ph^{602}/FRT19A,hs-FLP,tubP-GAL80;UAS-mCD8-GFP/GAL4-NP225*. Scale bar: 20 μm.

To examine further when distinct *ph* mutant neurons acquired the final uniform gene expression profile, we characterized both control and *ph* mosaic brains for patterns of MARCM clones at various pupal stages. When *GAL4-NP225* was used to label MARCM clones, we detected only clones of PNs in wild-type mosaic brains but started to observe multiple unrecognizable GAL4-positive clones in *ph* mosaic brains around 1-2 days APF (Fig. 5). We observe similar phenomena in the clones of *ph* mutant neurons that were induced at the mid-3rd instar stage (data not shown). All these results suggest that loss of neuronal diversity in *ph* mutant clones specifically occurs during early metamorphosis and probably because of induction of unpatterned ecdysone-mediated transcriptional hierarchies (see Discussion).

To determine directly the role of ecdysone in the transformation of *ph* mutant neurons during early metamorphosis, we subsequently examined whether and how synthetic 20-hydroxyecdysone affects MARCM labeling of *ph* mutant clones in cultured fly brains. We first found that loss of neuronal diversity, as evidenced by appearance of multiple unrecognizable MARCM clones, inevitably occurred in *ph* mosaic brains that were cultured from the late wandering larval stage (empty gut stage) (data not shown). By contrast, transformation of *ph* mutant neurons depended on the availability of 20-hydroxyecdysone when culture of mosaic brains started before larval wandering (Fig. 6). We cultured *ph* mosaic brains for 4 days and detected no sign for loss of neuronal diversity in the absence of 20-hydroxyecdysone (Fig. 6A). But adding 20-hydroxyecdysone into the media from the beginning or even 4 days later efficiently led to transformation of *ph* mutant clones and appearance of multiple bizarre GFP-positive clones in cultured *ph* mosaic brains (Fig. 6B,C). Such ecdysone-dependent changes in the patterns of MARCM clones were never observed in wild-type mosaic brains that were cultured in parallel (data not shown). These results provide direct evidence for involvement of ecdysone signaling in transforming *ph* mutant neurons of various origins into a homogeneous population of abnormal cells.

Differential involvement of distinct PcG proteins in neuronal development

Ph is best known for its involvement with other PcG proteins in maintaining the silent state of homeotic (Hox) genes (e.g. Beuchle et al., 2001; Choi et al., 2000). To determine roles of general PcG functions in neuronal development, we conducted loss-of-function mosaic analysis for two other PcG proteins, Polycomb (Pc) and Enhancer of zeste [E(z)]. Two distinct multimeric PcG complexes, which each contains different PcG proteins, have been identified (Levine et al., 2004). Multiple lines of evidence reveal that Ph forms complexes with Pc but not with E(z) (e.g. Franke et al., 1992; Shao et al., 1999). However, neither *Pc* nor *E(z)* mutant clones phenocopy Ph loss-of-function phenotypes (Fig. 7). First, we no longer observe ectopic expression of *GAL4-OK107* in the neuronal clones, that are normally negative for *GAL4-OK107* expression, within *Pc* or *E(z)* mosaic brains. This did help us identify variably deformed MB clones. Second, MB clones homozygous for these different PcG mutations exhibit distinct morphological anomalies. At the wandering larval stage, we specifically observe exuberant disorganized ‘dendrites’ in *Pc* Nb clones (arrow in Fig. 7A). Preferential involvement of Pc in confining dendritic growth is further evidenced by acquisition of over-elaborated dendrites, but not axons, in the single-cell clones of *Pc* mutant adult MB neurons (Fig. 7F compared with 7E). By contrast, no specific gross defect could be detected in either larval *E(z)* mutant Nb clones (Fig. 7B) or adult *E(z)* mutant single-cell clones (Fig. 7G). In addition, although both *Pc* (Fig. 7C) and *E(z)* (Fig. 7D) mutant MB Nb clones exhibit many ectopic neurites at the adult stage, the presence of calyx-like structures in the *E(z)* (inset in Fig. 7D), but not *Pc*, clones, together with significant reductions in the numbers of normal-projecting axons strongly suggest that the wide-spreading neurites are mostly misguided axons, but not overshooting exuberant dendrites, in the adult *E(z)* mutant Nb clones (Fig. 7D). Interestingly, such defasciculation of neurites is in great contrast with the aberrantly aggregated neuronal bundles of *Ph* mutant clones (compare Fig. 7C,D with Fig. 1D). Finally, we observe ectopic labeling of glia-like

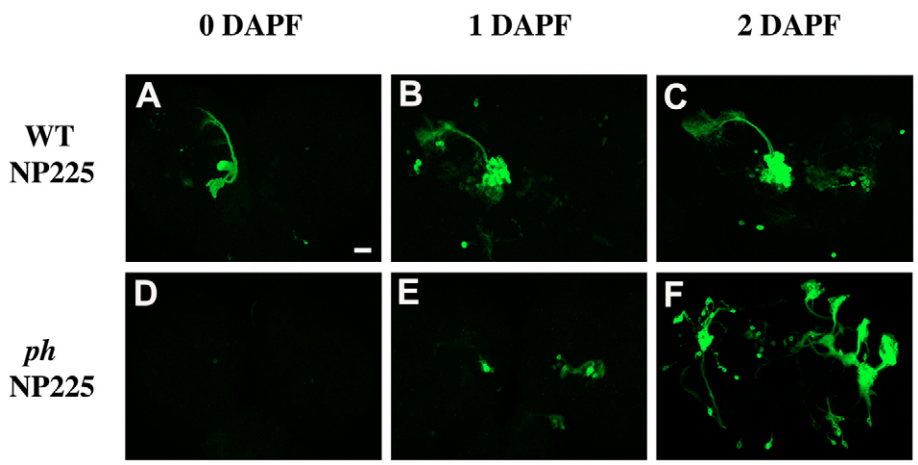

Fig. 5. Phenotypic analysis of *ph* mutant clones through puparium formation. Composite confocal images of mosaic fly brains fixed during puparium formation (0D APF), 1D APF or 2D APF. In wild-type mosaic brains, *GAL4-NP225* constantly labeled clones of projection neurons through pupal stages (**A-C**). By contrast, *GAL4-NP225* labeled many ectopic clones of *ph* mutant neurons after 2D APF (**D-F**). Genotypes: (A-C) *FRT19A/FRT19A,hs-FLP,tubP-GAL80;UAS-mCD8-GFP/GAL4-NP225*; (D-F) *FRT19A,ph^{602}/FRT19A,hs-FLP,tubP-GAL80;UAS-mCD8-GFP/GAL4-NP225*. Scale bar: 20 μm.

cells only in *E(z)* mutant mosaic adult brains (Fig. 7H). This phenomenon suggests selective involvement of E(z) in governing glial identity. Taken together, distinct PcG proteins are differentially involved in regulating various aspects of brain development, suggesting specific roles of Ph in maintaining neuronal diversity especially through metamorphosis.

Derepression of distinct Hox genes in different PcG mutant clones

Derepression of Hox genes has been implicated in the acquisition of abnormal cell fates by PcG mutant cells outside the nervous system (e.g. Choi et al., 2000; Beuchle et al., 2001). We wondered whether similar mechanisms underlie abnormal development of PcG mutant neurons. Using immunohistochemistry, we characterized expression of eight Hox genes, including *abd-A*, *abd-B*, *ubx*, *antp*, *pb*, *dfd*, *lab* and *scr*, in various PcG mutant clones at the wandering larval stage. Distinct Hox genes are normally expressed in different characteristic segmental domains. For example, expression of *abd-B* and *ubx* is restricted to the terminus and one middle segment of the ventral ganglion, respectively (Fig. 8A,H). Examining whether any Hox gene became ectopically expressed in mosaic larval CNSs, we found that only *abd-B* was misexpressed in *ph* mutant clones, while misexpression of several Hox genes, including *abd-A*, *abd-B* and *antp*, occurred in *Pc* mutant clones (Fig. 8; Table 1). Furthermore, when we ectopically expressed *abd-B* in wild-type MARCM clones using *GAL4-C155/UAS-abd-B*, no obvious defects were found in the axonal projection patterns of various neurons (J.W., C.-H.J.L. and T.L., unpublished). These results suggest little involvement of Hox genes in the unanimously abnormal responses of *ph* mutant neurons to ecdysone signaling during early metamorphosis. In addition, only *antp* became derepressed when *E(z)* was knocked out; and derepression of *antp* was restricted to about 20% of *E(z)* mutant clones (Table 1). Taken together, derepression of distinct Hox genes occurs in different PcG mutant clones, further suggesting differential involvement of distinct PcG proteins in governing neuronal identities through development.

DISCUSSION

Ph is well implicated in maintaining cell fates via controlling transcription of genes in distinct cell type-characteristic manners (e.g. Dura and Ingham, 1988). Deregulation of multiple genes aberrantly occurs in *ph* mutant tissues (e.g. Dura and Ingham, 1988; Beuchle et al., 2001). A similar mechanism probably underlies most of the abnormalities in *ph* mutant neurons. In particular, there are multiple lines of evidence suggesting mal-expression of various subtype-specific GAL4 drivers in *ph* mutant clones. First, with respect to GAL4-OK107, GAL4-NP225 and elav-GAL4, the use of various GAL4 drivers results in labeling of similar numbers of clones (Fig. 3M-O). Second, we observe clones in the central brain versus the optic lobe, depending on when mitotic recombination is induced (compare Fig. 3N-O with Fig. 4C-D), which is the same as in wild-type mosaic brains (compare Fig. 3B with Fig. 4A). Third, ato-GAL4 and GAL4-EB1 fail to label any clone (Fig. 3P, data not shown for GAL4-EB1), arguing against constitutive expression of UAS-transgenes in mutant clones. Finally, examining clones through development reveals no evidence for derivation of some clones from other clones; and, instead, we constantly observe sudden labeling of full-sized clones shortly after a big ecdysone pulse (Fig. 5). Apparently, loss of Ph function alone is short of causing the full spectrum of abnormalities. Mass ecdysone is required for the

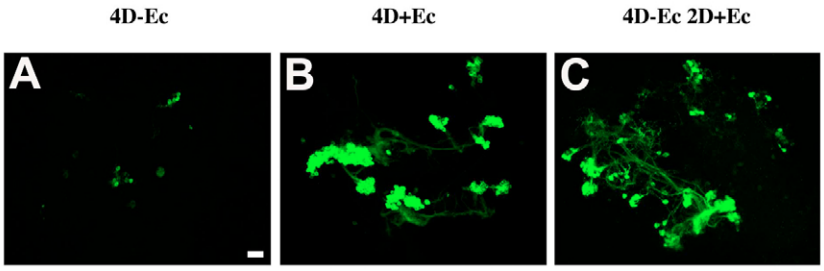

Fig. 6. Ecdysone-dependent transformation of *ph* mutant neurons in cultured mosaic larval brains. Composite confocal images of variably cultured larval brains that contain clones of *ph* mutant neurons with *GAL4-OK107* as a driver. Few GFP-positive cells exist after 4 days of culture in the absence of 20-hydroxyecdysone (**A**). By contrast, there are many GFP-positive cells when ecdysone was added at the beginning (**B**) or on the fifth day of the culture (**C**). Genotype: *FRT19A/FRT19A,hs-FLP,tubP-GAL80;UAS-mCD8-GFP/+;GAL4-OK107/+*. Scale bar: 20 μm.

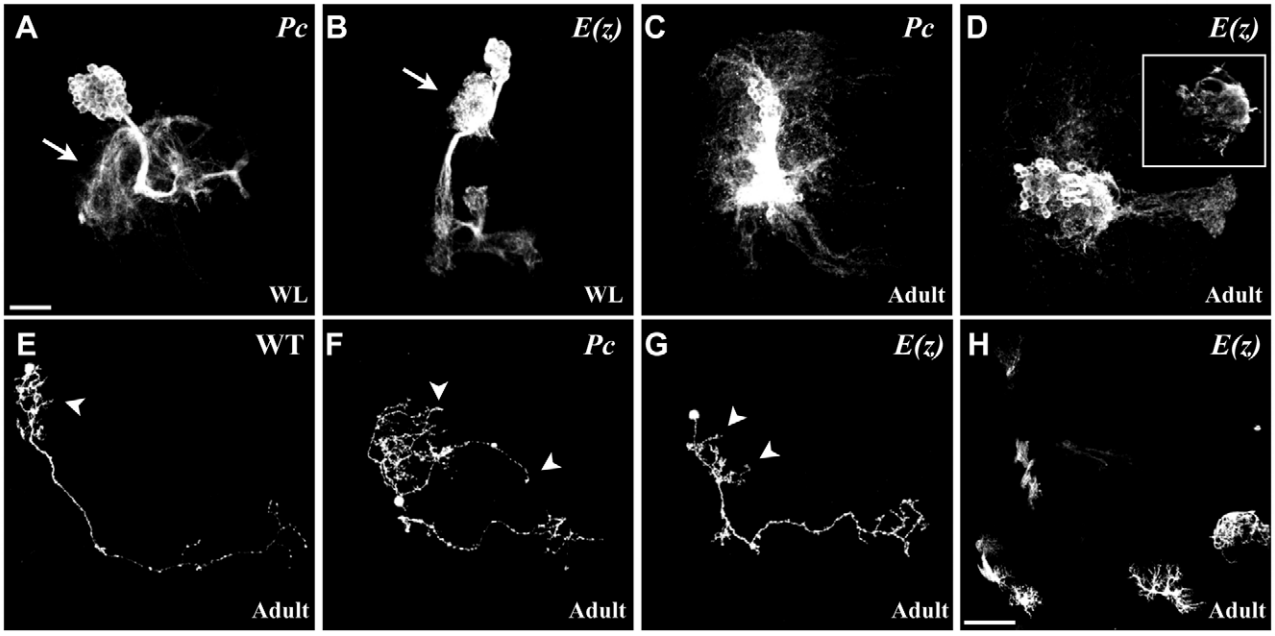

Fig. 7. MARCM analysis of *Pc* and *E(z)* in the mosaic fly brains. (**A-G**) Composite confocal images of various MB clones at the wandering larval (A,B) or adult (C-G) stage. A gigantic loose structure is present in the larval *Pc* mutant Nb clone (arrow in A) versus the dense well-defined calyx in the larval *E(z)* mutant Nb clone (arrow in B). Numerous ectopic neurites are present in both *Pc* (C) and *E(z)* (D) mutant adult Nb clones, and the dendritic tree is over-elaborated in the adult *Pc* single-cell clone (arrowhead in F; compare with arrowheads in E and G). A calyx-like structure in the adult *E(z)* mutant Nb clone is shown in the inset in D. (**H**) Various glia-like *E(z)* mutant brain cells became ectopically labeled by *GAL4-OK107*. Genotypes: (A,C,F) hs-FLP,UAS-mCD8GFP/+; Pc^{XT109},FRT2A/tubP-GAL80,FRT2A;GAL4-OK107/+; (B,D,G,H) hs-FLP,UAS-mCD8GFP/+;$E(z)^{731}$,FRT2A/tubP-GAL80,FRT2A;GAL4-OK107/+; and (E) hs-FLP,UAS-mCD8GFP/+;FRT2A/tubP-GAL80,FRT2A;GAL4-OK107/+. Scale bar: 20 μm.

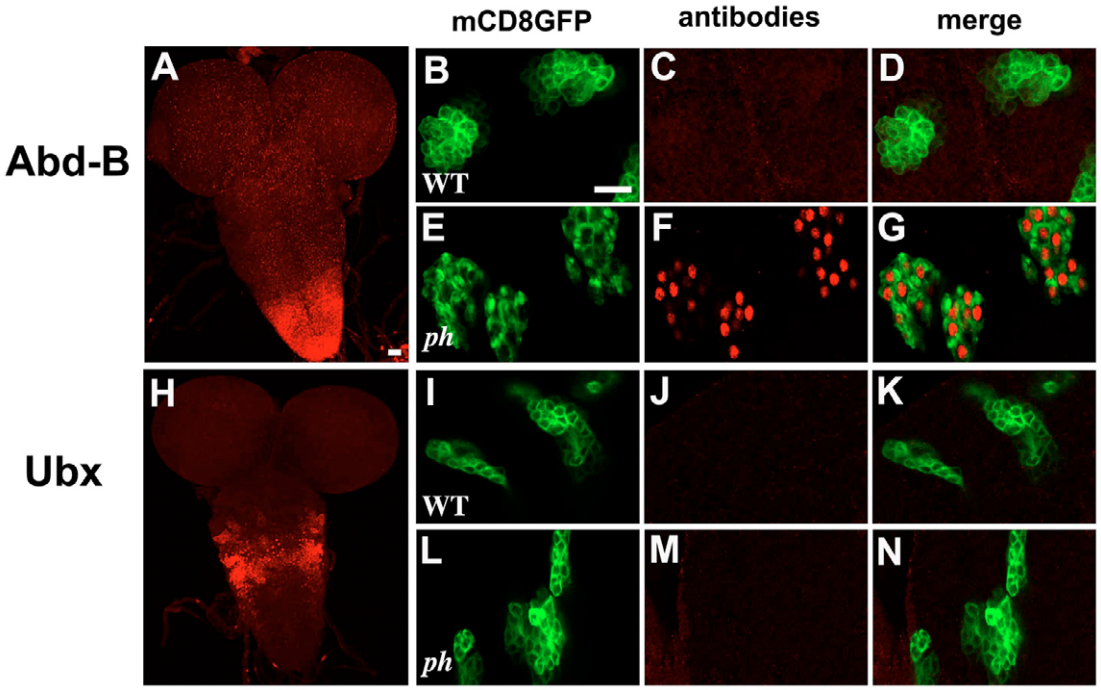

Fig. 8. Derepression of *abd-B* in clones of *ph* mutant neurons. Composite confocal images of whole wandering larval CNSs (**A**,**H**) and MARCM clones of wild-type (**B-D**,**I-K**) or *ph* mutant (**E-G**,**L-N**) neurons in the central brains of wandering larvae. Green shows MARCM clones that are positive for mCD8-GFP (B,E,I,L), red shows anti-Abd-B (A,C,F) or anti-Ubx (H,J,M). (D,G,K,N) Merged images. (A-G) Endogenous Abd-B is restricted to the terminal one-third of the ventral ganglion (A), and ectopic expression of *abd-B* in MARCM clones of *ph* mutant neurons (compare F and G with C and D). (H-N) By contrast, endogenous Ubx is enriched in the middle segment of the ventral ganglion (H) and no ectopic expression of Ubx is detected (I-N). Genotypes: (A,H) wild type; (B-D,I-K) *FRT19A/FRT19A,hs-FLP,tubP-GAL80;UAS-mCD8-GFP/+;elav-GAL4/+*; (E-G,L-N) *FRT19A,*ph^{602}*/FRT19A,hs-FLP,tubP-GAL80;UAS-mCD8-GFP/+;elav-GAL4/+*. Scale bar: 20 μm.

Table 1. Derepression of Hox genes in the mutant clones of PcG genes

	abd-A	*abd-B*	*ubx*	*antp*	*pb*	*Dfd*	*lab*	*scr*
ph	–	+	–	–	–	–	–	–
Pc	+	+	–	+	–	–	–	–
E(z)	–	–	–	+/–*	–	–	–	–

**Antp* is ectopically expressed in about 20% of *E(z)* mutant neuronal clones.

pathological transformation of *ph* mutant neurons in the *Drosophila* brain, raising several interesting possibilities about mutual involvement between the epigenetic function of PcG and the global nuclear signaling of steroid hormones.

Distinct wild-type cells respond differentially to ecdysone (e.g. Thummel et al., 1990; Truman et al., 1994; Bender et al., 1997; Lee et al., 2000), but *ph* mutant neurons of distinct origins become no longer distinguishable after ecdysone signaling. Ecdysone mediates diverse biological activities partially via binding to different heterodimeric receptors (e.g. Schubiger et al., 1998; Lee et al., 2000; Cherbas et al., 2003). Its conventional receptors consist of the nuclear receptor superfamily members ecdysone receptor (EcR) and Ultraspiracle (USP; the *Drosophila* RXR) (Yao et al., 1992; Yao et al., 1993). There are three documented EcR isoforms (Talbot et al., 1993); and cells that express different EcR isoforms have been shown to undergo different changes in response to the prepupal ecdysone peak (Truman et al., 1994). For example, abundant EcR-B1 exists selectively in the neurons that remodel projections during early metamorphosis (Schubiger et al., 1998; Lee et al., 2000). As we detected no change in EcR expression patterns in *ph* mutant neurons (J.W., C.-H.J.L. and T.L., unpublished), it is unlikely that the aberrant responses of *ph* mutant neurons to the prepupal ecdysone peak occur as a result of derepression of specific EcR isoforms. In addition, derepression of multiple Hox genes appears not involved either. Nevertheless, given the involvement of Ph in silencing transcription, it remains possible that derepression of other unidentified genes directly re-programs ecdysone-induced transcriptional hierarchies, leading to transformation of *ph* mutant neurons. Alternatively, it is possible that loss of the epigenetic function of Ph may permit diffuse activation of prohibited genes by normal transcriptional hierarchies. Moreover, massive steroid hormone signaling might directly modify genomic imprinting when PcG functions are compromised.

It is generally thought that nuclear signaling of steroid hormones occurs routinely through the life of an organism without affecting the memories of most cells. However, high levels of sex hormones during pregnancy possibly alter gene expression patterns permanently in the mammary gland even after involution (Ginger et al., 2001). Exposure to some hormonally active reagents during early development also has the potential for imprinting long-lasting changes on the action of related hormones (Mena et al., 1992). In mammalian neurons, the estrogen receptor-α was further found to silence gene expression in an epigenetic fashion and via hypermethylation of the involved promoters (Zschocke et al., 2002). All these phenomena argue for the abilities of steroid hormones to modulate genomic imprint, at least, under certain circumstances. Ecdysone-dependent transformation of *ph* mutant neurons, thus, provides a possible model system for characterizing the epigenetic functions of steroid hormones in genetically malleable organisms. In addition, our demonstration of the unusual potent epigenetic effects of ecdysone in *ph* mutant neurons suggests complex mechanisms may underlie pathogenesis of other documented PcG loss-of-function phenotypes.

Both derepression and inactivation of genes occur in transformed *ph* mutant neurons, characterization of which offers some molecular insights into this status of transformation. First, we no longer detected the fine-tuning of gene expression in transformed cells; and all the examined drivers appeared either fully on or completely off. Second, on or off could not be simply attributed to the genomic locations of drivers, as evidenced by constitutive silencing of the multiple independently inserted *atonal-GAL4* transgenes. Third, transformed cells retained neuron-type morphologies and remained positive for the neuron-specific gene *elav*; and *ph* mutant neurons had been earlier reported to acquire normal-looking neurites in culture (Smouse and Perrimon, 1990). Taken together, the transformation leads to loss of subtype identity without affecting basic neuronal fates, abolishes the genomic imprints governing fine controls over gene expression, and locks gene expression in 'on' or 'off' possibly in a promoter-autonomous manner (largely independent of its chromatin environment).

Finally, loss of Ph, Pc, versus E(z) results in distinct phenotypes in the developing fly brain. Differences in their underlying pathological mechanisms are well exemplified by differential derepression of distinct Hox genes in different PcG clones. In addition, for a given PcG mutation, patterns of Hox gene derepression vary from neural clones to wing disc clones (Beuchle et al., 2001) and visceral mesoderm (Choi et al., 2000). It remains to be elucidated how distinct PcG functions are governed in diverse cell type-characteristic manners.

We are grateful to J. Müller for *Pc* and *E(z)* mutations, to N. B. Randsholt for *P{ph-d+}* transgene, to K. Ito and H. Bellen for *GAL4-NP225* and *ato-GAL4*, and to T. Kaufman, I. Duncan and J. Müller for antibodies against Hox proteins. We also thank P. Jones for critically reading the manuscript. This work is supported by the National Institutes of Health. T.L. is a Klingenstein Fellow.

References

Bender, M., Imam, F. B., Talbot, W. S., Ganetzky, B. and Hogness, D. S. (1997). Drosophila ecdysone receptor mutations reveal functional differences among receptor isoforms. *Cell* **91**, 777-788.

Beuchle, D., Struhl, G. and Muller, J. (2001). Polycomb group proteins and heritable silencing of Drosophila Hox genes. *Development* **128**, 993-1004.

Bienz, M. and Muller, J. (1995). Transcriptional silencing of homeotic genes in Drosophila. *BioEssays* **17**, 775-784.

Bloyer, S., Cavalli, G., Brock, H. W. and Dura, J. M. (2003). Identification and characterization of polyhomeotic PREs and TREs. *Dev. Biol.* **261**, 426-442.

Boivin, A. and Dura, J. M. (1998). In vivo chromatin accessibility correlates with gene silencing in Drosophila. *Genetics* **150**, 1539-1549.

Boivin, A., Fauvarque, M. O. and Dura, J. M. (1999). One-to-one correspondence between the two genetic units and the tandemly duplicated transcriptional units of the polyhomeotic locus of Drosophila. *Mol. Gen. Genet.* **261**, 196-200.

Briscoe, J., Pierani, A., Jessell, T. M. and Ericson, J. (2000). A homeodomain protein code specifies progenitor cell identity and neuronal fate in the ventral neural tube. *Cell* **101**, 435-445.

Brock, H. W. and van Lohuizen, M. (2001). The Polycomb group – no longer an exclusive club? *Curr. Opin. Genet. Dev.* **11**, 175-181.

Campbell, R. B., Sinclair, D. A., Couling, M. and Brock, H. W. (1995). Genetic interactions and dosage effects of Polycomb group genes of Drosophila. *Mol. Gen. Genet.* **246**, 291-300.

Cherbas, L., Hu, X., Zhimulev, I., Belyaeva, E. and Cherbas, P. (2003). EcR isoforms in Drosophila: testing tissue-specific requirements by targeted blockade and rescue. *Development* **130**, 271-284.

Choi, S. H., Oh, C. T., Kim, S. H., Kim, Y. T. and Jeon, S. H. (2000). Effects of Polycomb group mutations on the expression of Ultrabithorax in the Drosophila visceral mesoderm. *Mol. Cells* **10**, 156-161.

Connolly, J. B., Roberts, I. J., Armstrong, J. D., Kaiser, K., Forte, M., Tully, T. and O'Kane, C. J. (1996). Associative learning disrupted by impaired Gs signaling in Drosophila mushroom bodies. *Science* **274**, 2104-2107.

Deatrick, J., Daly, M., Randsholt, N. B. and Brock, H. W. (1991). The complex genetic locus polyhomeotic in Drosophila melanogaster potentially encodes two homologous zinc-finger proteins. *Gene* **105**, 185-195.

DeCamillis, M., Cheng, N. S., Pierre, D. and Brock, H. W. (1992). The polyhomeotic gene of Drosophila encodes a chromatin protein that shares polytene chromosome-binding sites with Polycomb. *Genes Dev.* **6**, 223-232.

Doe, C. Q. and Skeath, J. B. (1996). Neurogenesis in the insect central nervous system. *Curr. Opin. Neurobiol.* **6**, 18-24.
Duncan, I. M. (1982). Polycomblike: a gene that appears to be required for the normal expression of the bithorax and antennapedia gene complexes of Drosophila melanogaster. *Genetics* **102**, 49-70.
Dura, J. M. and Ingham, P. (1988). Tissue- and stage-specific control of homeotic and segmentation gene expression in Drosophila embryos by the polyhomeotic gene. *Development* **103**, 733-741.
Dura, J. M., Randsholt, N. B., Deatrick, J., Erk, I., Santamaria, P., Freeman, J. D., Freeman, S. J., Weddell, D. and Brock, H. W. (1987). A complex genetic locus, polyhomeotic, is required for segmental specification and epidermal development in D. melanogaster. *Cell* **51**, 829-839.
Fitzgerald, D. P. and Bender, W. (2001). Polycomb group repression reduces DNA accessibility. *Mol. Cell. Biol.* **21**, 6585-6597.
Forlani, S., Lawson, K. A. and Deschamps, J. (2003). Acquisition of Hox codes during gastrulation and axial elongation in the mouse embryo. *Development* **130**, 3807-3819.
Franke, A., DeCamillis, M., Zink, D., Cheng, N., Brock, H. W. and Paro, R. (1992). Polycomb and polyhomeotic are constituents of a multimeric protein complex in chromatin of Drosophila melanogaster. *EMBO J.* **11**, 2941-2950.
Gibbs, S. M. and Truman, J. W. (1998). Nitric oxide and cyclic GMP regulate retinal patterning in the optic lobe of Drosophila. *Neuron* **20**, 83-93.
Ginger, M. R., Gonzalez-Rimbau, M. F., Gay, J. P. and Rosen, J. M. (2001). Persistent changes in gene expression induced by estrogen and progesterone in the rat mammary gland. *Mol. Endocrinol.* **15**, 1993-2009.
Gould, A. (1997). Functions of mammalian Polycomb group and trithorax group related genes. *Curr. Opin. Genet. Dev.* **7**, 488-494.
Hassan, B. A., Bermingham, N. A., He, Y., Sun, Y., Jan, Y. N., Zoghbi, H. Y. and Bellen, H. J. (2000). atonal regulates neurite arborization but does not act as a proneural gene in the Drosophila brain. *Neuron* **25**, 549-561.
Horard, B., Tatout, C., Poux, S. and Pirrotta, V. (2000). Structure of a polycomb response element and in vitro binding of polycomb group complexes containing GAGA factor. *Mol. Cell. Biol.* **20**, 3187-3197.
Ito, K., Awano, W., Suzuki, K., Hiromi, Y. and Yamamoto, D. (1997). The Drosophila mushroom body is a quadruple structure of clonal units each of which contains a virtually identical set of neurones and glial cells. *Development* **124**, 761-771.
Jacob, J. and Briscoe, J. (2003). Gli proteins and the control of spinal-cord patterning. *EMBO Rep.* **4**, 761-765.
Jefferis, G. S., Marin, E. C., Stocker, R. F. and Luo, L. (2001). Target neuron prespecification in the olfactory map of Drosophila. *Nature* **414**, 204-208.
Jurgens, G. (1985). A group of genes controlling the spatial expression of the bithorax complex in Drosophila. *Nature* **316**, 153-155.
Lee, T. and Luo, L. (1999). Mosaic analysis with a repressible cell marker for studies of gene function in neuronal morphogenesis. *Neuron* **22**, 451-461.
Lee, T., Lee, A. and Luo, L. (1999). Development of the Drosophila mushroom bodies: sequential generation of three distinct types of neurons from a neuroblast. *Development* **126**, 4065-4076.
Lee, T., Marticke, S., Sung, C., Robinow, S. and Luo, L. (2000). Cell autonomous requirement of the USP/EcR-B ecdysone receptor for mushroom body neuronal remodeling. *Neuron* **28**, 807-818.
Levine, S. S., King, I. F. and Kingston, R. E. (2004). Division of labor in Polycomb group repression. *Trends Biochem. Sci.* **29**, 478-485.
Lewis, E. B. (1978). A gene complex controlling segmentation in Drosophila. *Nature* **276**, 565-570.
Lin, D. M. and Goodman, C. S. (1994). Ectopic and increased expression of Fasciclin II alters motoneuron growth cone guidance. *Neuron* **13**, 507-523.
Luo, L., Liao, Y. J., Jan, L. Y. and Jan, Y. N. (1994). Distinct morphogenetic functions of similar small GTPases: Drosophila Drac1 is involved in axonal outgrowth and myoblast fusion. *Genes Dev.* **8**, 1787-1802.
McGinnis, W. and Krumlauf, R. (1992). Homeobox genes and axial patterning. *Cell* **68**, 283-302.
Mena, M. A., Arriaza, C. A. and Tchernitchin, A. N. (1992). Early postnatal androgenization imprints selective changes in the action of estrogens in the rat uterus. *Biol. Reprod.* **46**, 1080-1085.
Muller, J. (1995). Transcriptional silencing by the Polycomb protein in Drosophila embryos. *EMBO J.* **14**, 1209-1220.
Narbonne, K., Besse, F., Brissard-Zahraoui, J., Pret, A. M. and Busson, D. (2004). polyhomeotic is required for somatic cell proliferation and differentiation during ovarian follicle formation in Drosophila. *Development* **131**, 1389-1400.
Ng, J., Hart, C. M., Morgan, K. and Simon, J. A. (2000). A Drosophila ESC-E(Z) protein complex is distinct from other polycomb group complexes and contains covalently modified ESC. *Mol. Cell. Biol.* **20**, 3069-3078.
Orlando, V. (2003). Polycomb, epigenomes, and control of cell identity. *Cell* **112**, 599-606.
Perrimon, N., Engstrom, L. and Mahowald, A. P. (1985). Developmental genetics of the 2C-D region of the Drosophila X chromosome. *Genetics* **111**, 23-41.
Peter, A., Schottler, P., Werner, M., Beinert, N., Dowe, G., Burkert, P., Mourkioti, F., Dentzer, L., He, Y., Deak, P. et al. (2002). Mapping and identification of essential gene functions on the X chromosome of Drosophila. *EMBO Rep.* **3**, 34-38.
Pirrotta, V. (1998). Polycombing the genome: PcG, trxG, and chromatin silencing. *Cell* **93**, 333-336.
Randsholt, N. B., Maschat, F. and Santamaria, P. (2000). *polyhomeotic* controls *engrailed* expression and the *hedgehog* signaling pathway in imaginal discs *Mech. Dev.* **95**, 89-99.
Ringrose, L., Rehmsmeier, M., Dura, J. M. and Paro, R. (2003). Genome-wide prediction of Polycomb/Trithorax response elements in Drosophila melanogaster. *Dev. Cell* **5**, 759-771.
Saget, O. and Randsholt, N. B. (1994). Transposon-induced rearrangements in the duplicated locus ph of Drosophila melanogaster can create new chimeric genes functionally identical to the wild type. *Gene* **149**, 227-235.
Saurin, A. J., Shao, Z., Erdjument-Bromage, H., Tempst, P. and Kingston, R. E. (2001). A Drosophila Polycomb group complex includes Zeste and dTAFII proteins. *Nature* **412**, 655-660.
Schmid, A., Chiba, A. and Doe, C. Q. (1999). Clonal analysis of Drosophila embryonic neuroblasts: neural cell types, axon projections and muscle targets. *Development* **126**, 4653-4689.
Schubiger, M., Wade, A. A., Carney, G. E., Truman, J. W. and Bender, M. (1998). Drosophila EcR-B ecdysone receptor isoforms are required for larval molting and for neuron remodeling during metamorphosis. *Development* **125**, 2053-2062.
Shao, Z., Raible, F., Mollaaghababa, R., Guyon, J. R., Wu, C. T., Bender, W. and Kingston, R. E. (1999). Stabilization of chromatin structure by PRC1, a Polycomb complex. *Cell* **98**, 37-46.
Simon, J., Chiang, A. and Bender, W. (1992). Ten different Polycomb group genes are required for spatial control of the abdA and AbdB homeotic products. *Development* **114**, 493-505.
Smouse, D. and Perrimon, N. (1990). Genetic dissection of a complex neurological mutant, polyhomeotic, in Drosophila. *Dev. Biol.* **139**, 169-185.
Smouse, D., Goodman, C., Mahowald, A. and Perrimon, N. (1988). polyhomeotic: a gene required for the embryonic development of axon pathways in the central nervous system of Drosophila. *Genes Dev.* **2**, 830-842.
Talbot, W. S., Swyryd, E. A. and Hogness, D. S. (1993). Drosophila tissues with different metamorphic responses to ecdysone express different ecdysone receptor isoforms. *Cell* **73**, 1323-1337.
Thummel, C. S., Burtis, K. C. and Hogness, D. S. (1990). Spatial and temporal patterns of E74 transcription during Drosophila development. *Cell* **61**, 101-111.
Truman, J. W., Talbot, W. S., Fahrbach, S. E. and Hogness, D. S. (1994). Ecdysone receptor expression in the CNS correlates with stage-specific responses to ecdysteroids during Drosophila and Manduca development. *Development* **120**, 219-234.
Urbach, R., Schnabel, R. and Technau, G. M. (2003). The pattern of neuroblast formation, mitotic domains and proneural gene expression during early brain development in Drosophila. *Development* **130**, 3589-3606.
Wang, J., Zugates, C. T., Liang, I. H., Lee, C.-H. J. and Lee, T. (2002). Drosophila Dscam is required for divergent segregation of sister branches and suppresses ectopic bifurcation of axons. *Neuron* **33**, 559-571.
Yao, T. P., Segraves, W. A., Oro, A. E., McKeown, M. and Evans, R. M. (1992). Drosophila ultraspiracle modulates ecdysone receptor function via heterodimer formation. *Cell* **71**, 63-72.
Yao, T. P., Forman, B. M., Jiang, Z., Cherbas, L., Chen, J. D., McKeown, M., Cherbas, P. and Evans, R. M. (1993). Functional ecdysone receptor is the product of EcR and Ultraspiracle genes. *Nature* **366**, 476-479.
Zheng, X., Wang, J., Haerry, T. E., Wu, A. Y.-H., Martin, J., O'Connor, M. B., Lee, C.-H. J. and Lee, T. (2003). TGF-beta signaling activates steroid hormone receptor expression during neuronal remodeling in the Drosophila brain. *Cell* **112**, 303-315.
Zhong, W. (2003). Diversifying neural cells through order of birth and asymmetry of division. *Neuron* **37**, 11-14.
Zink, D. and Paro, R. (1995). Drosophila Polycomb-group regulated chromatin inhibits the accessibility of a trans-activator to its target DNA. *EMBO J.* **14**, 5660-5671.
Zschocke, J., Manthey, D., Bayatti, N., van der Burg, B., Goodenough, S. and Behl, C. (2002). Estrogen receptor alpha-mediated silencing of caveolin gene expression in neuronal cells. *J. Biol. Chem.* **277**, 38772-38780.